Sinking rates of microplastics and potential implications of their alteration by physical, biological, and chemical factors

CrossMark

Nicole Kowalski *, Aurelia M. Reichardt, Joanna J. Waniek

Leibniz Institute for Baltic Sea Research Warnemuende, Seestraße 15, 18119 Rostock, Germany

ABSTRACT

To follow the pathways of microplastics in aquatic environments, profound knowledge about the behaviour of microplastics is necessary. Therefore, sinking experiments were conducted with diverse polymer particles using fluids with different salinity. Particles ranged from 0.3 and 3.6 mm with sinking rates between 6 and 91×10^{-3} ms^{-1}. The sinking velocity was not solely related to particle density, size and fluid density but also to the particles shape leading to considerable deviation from calculated theoretical values. Thus, experimental studies are indispensable to get basic knowledge about the sinking behaviour and to gain representative datasets for model approaches estimating the distribution of microplastics in aquatic systems. The sinking behaviour may be altered considerably by weathering and biofouling demanding further studies with aged and fouled plastic particles. Furthermore, assumptions are made about the influence of sinking fouled microplastics on the marine carbon pump by transferring organic carbon to deeper water depths.

© 2016 Elsevier Ltd. All rights reserved.

1. Introduction

During the last 50 years plastic production increased dramatically being coupled with a worldwide release of plastic waste to the environment (e.g. Barnes et al., 2009). The distribution and accumulation of plastic debris in aquatic environments has been observed internationally with growing concern, forcing the action of governments and industry (Galgani et al., 2013). Thus, environmental monitoring and assessment enhancing the knowledge about the extent and impact of plastic debris are necessary for political decisions and guidance. This especially includes very small plastic pieces (Galgani et al., 2013; GESAMP, 2015).

Small plastic debris, defined as microplastics in a size range of <5 mm (Barnes et al., 2009), is distributed worldwide in aquatic ecosystems (Derraik, 2002; Ivar do Sul and Costa, 2007; Cole et al., 2011; Eriksen et al., 2014). Particles have been found in the water column (e.g. Thiel et al., 2003; Sadri and Thompson, 2014; Zhao et al., 2014), coastal sediments (e.g. Claessens et al., 2011; Liebezeit and Dubaish, 2012; van Cauwenberghe et al., 2013, 2014; Stolte et al., 2015) as well as in marine organisms which ingest them with their nourishment (e.g. Boerger et al., 2010; Davison and Asch, 2011; Cole et al., 2013). When released into the environment by waste water, ship traffic, harbour activities or fragmentation of large plastic debris (Derraik, 2002) microplastics cannot yet be removed. It is assumed to take decades or centuries to decompose the resistant plastic debris (e.g. Shaw and

Day, 1994; Barnes et al., 2009). Meanwhile, the debris is fragmenting continuously into smaller pieces (Andrady, 2011) thereby becoming even available to zooplankton (Cole et al., 2013; Desforges et al., 2015). Fragmentation by mechanical action is supported by photodegradation which leads to the embrittlement of polymers (Pegram and Andrady, 1989). Degradation by microorganisms seems to play a minor role as most of the polymers are resistant against biodegradation (Thompson et al., 2005). However, polymer additives which often consist of hazardous substances (organic pollutants, heavy metals) may be liberated quite fast during the aging of plastic debris (Dimitrakakis et al., 2009; Teuten et al., 2009; Lithner et al., 2011; Koelmans et al., 2014). Further potential risks are posed by hazardous compounds adsorbing to particle surfaces (Mato et al., 2000; Endo et al., 2005; Teuten et al., 2009; Bakir et al., 2012, 2014; Holmes et al., 2012; Turner and Holmes, 2015) and/or pathogenic microorganisms colonising the microplastics (Zettler et al., 2013; McCormick et al., 2014; Oberbeckmann et al., 2015) and being spread with the particles in the aquatic environment (Barnes and Milner, 2005).

To identify the ecological problems caused by microplastics it is essential to understand their pathways in the aquatic environment, their sources and sinks and how they are impacting the ecosystem (Browne et al., 2011). Thus, a substantial knowledge about the physical behaviour of microplastics is necessary. Until now, little is known about the sinking behaviour of microplastic particles (Wang et al., 2016). Ballent et al. (2013) presented first data on the sinking rates of high density plastic debris collected at beaches in Los Angeles (CA) with a mean diameter of 4.7 mm and an average sinking velocity of 28 mm s^{-1}. The sinking is mostly related to the particle density. Microplastics with

* Corresponding author.
E-mail address: nicole.kowalski@io-warnemuende.de (N. Kowalski).

densities higher than seawater settle down while particles with lower densities float at or near the sea surface (Barnes et al., 2009; Long et al., 2015). However, hydrodynamic conditions (e.g. river outflow, wind stress, and tidal forces) can influence the transport and distribution of microplastics significantly as shown e.g. by Browne et al. (2010), Collignon et al. (2012) and Ballent et al. (2013). Implementing the data from experimental studies of the sinking velocities into model approaches which simulate the hydrodynamic conditions helps to understand the pathways of microplastics in an aquatic system (Kukulka et al., 2012; Ballent et al., 2013). However, the particle density can be altered by weathering and biofouling (Morét-Ferguson et al., 2010). Especially colonisation of microorganisms have a ballasting effect on the particles resulting in the sinking of floating particles (Lobelle and Cunliffe, 2011; Cózar et al., 2014). Furthermore, microplastics can be incorporated in phytoplankton aggregates or faecal pellets enabling its transport to greater water depths and the seafloor and changing the density and sinking rates of aggregates and faecal pellets markedly (Cole et al., 2013, 2016; Long et al., 2015).

To contribute to the knowledge about the behaviour of microplastics in aquatic systems, sinking velocities of plastic particles with diverse densities were studied experimentally in water with different salinity. Additionally, the effects of weathering processes (UV irradiation, mechanical stress) on the particles were investigated. Results shall prospectively be implemented in a model approach tracing the distribution and residence of microplastics in the water column and sediments of the Baltic Sea.

2. Material and methods

2.1. Sinking experiments

2.1.1. Particle preparation

For the sinking experiments the polymer types polystyrene (PS, material density 1050 kg m^{-3}), polyamide (PA, 1140 kg m^{-3}), polymethyl methacrylate (PMMA, 1190 kg m^{-3}), polyethylene terephthalate (PET, 1390 kg m^{-3}), polyoxymethylene (POM, 1420 kg m^{-3}), and polyvinyl chloride (PVC, 1560 kg m^{-3}) were used. Virgin plastic pellets, which were provided by diverse polymer compounders (Table 1), were comminuted by the Department of Mineral Processing of the Brandenburg University of Technology Cottbus-Senftenberg (BTU) to gain particles <5 mm. For preparation an ultracentrifuge mill (ZM 200) in combination with a CryoMill (both Retsch GmbH, Germany) were used. Firstly the virgin pellets were frozen with liquid nitrogen, than pre-crushed with the ultracentrifuge mill using a 2 mm sieve and frequently cooled with liquid nitrogen. Secondary crushing was done batchwise (5 g, 64 g ball) with the Cryo-Mill under continuous cooling. Both mill systems were cooled with liquid nitrogen to freeze and embrittle the soft and flexile pellets and to prohibit smelting processes during the communition. This preparation process grinds the material into smaller pieces without changing its physical and chemical properties.

For the determination of the individual particles sizes a stereo microscope (SteREO Discovery.V8, Carl Zeiss, Germany) with coupled imaging software (AxioVision, Release 4.8.2 – SP2) was used. As the particles were of irregular shape (Fig. 1) an equivalent spherical diameter (ESD) was calculated on the basis of a best-fit ellipse using the measured major (a), minor (b) and intermediate (c) axes as defined by Kumar et al. (2010):

$$ESD = (abc)^{\frac{1}{3}} \tag{1}$$

For the calculation of the ESD of the more cylindrical PS particles (Fig. 1a) the following formula for cylinders was used:

$$ESD = 2\left(\frac{3}{4}r^2h\right)^{\frac{1}{3}} \tag{2}$$

with r = radius and h = height of the cylindrical particle.

For the description of the particles shapes Krumbein's Spheri-city Index (Krumbein, 1941) and Cailleux's Flatness Index (Cailleux, 1945), usually used in sedimentary petrology to characterise the grain shape of rocks, were calculated (Table 1).

2.1.2. Measurement of sinking rates

The sinking experiments were performed in a temperature controlled room (ca. 20 °C) using three uniform settling columns (Atterberg cylinders, 40 cm length, 7.5 cm in diameter) filled with deionised water (Sal 0, density 998 kg m^{-3}), Baltic seawater (Sal 15, density 1010 kg m^{-3}, taken at the Warnow River outlet in Warnemünde) and Atlantic seawater (Sal 36, density 1026 kg m^{-3}, sampled in the Madeira Basin, North Atlantic). Before usage, the natural seawater was filtered through glass fibre filters (GFF, Whatman, pore size 0.7 μm) to remove the suspended particulate matter. Before beginning the sinking experiment the plastic particles were immersed in water of the same salinity and temperature used in the experiment. This was done to avoid electrostatic discharge at the particle surfaces, which may hamper subsidence of the particles. Particles were then transferred into the experimental water column with tweezers stopping the time the particle needed to cross two times a distance of 10 cm. Time recording started 15 cm below the artificial water surface to ensure that the particles reached their terminal velocity. With the measured sinking time and defined distance the sinking velocity of the individual particles was calculated.

2.1.3. Validation of measured sinking rates

The measured sinking velocities were validated by using perfectly round reference spheres made of polystyrene and with certified mean diameters of 0.5 mm ± 0.01 mm (density 1050 kg m^{-3}, Duke Standards, NIST Traceable Mean diameter, Thermo Fisher Scientific, Germany) and 1.98 mm ± 0.03 mm (density 1055 kg m^{-3}, PSS, Cospheric LLC, USA). Results were compared to theoretical sinking velocities (theor.

Table 1
Overview about the polymers used in the experiments containing information about the polymer suppliers and polymer types, particle density, particle number, size range (min–max, expressed as ESD), Krumbein's Sphericity Index indicating mean (min–max) (Krumbein, 1941), Cailleux's Flatness Index displaying mean (min–max) (Cailleux, 1945), and a description of the shape.

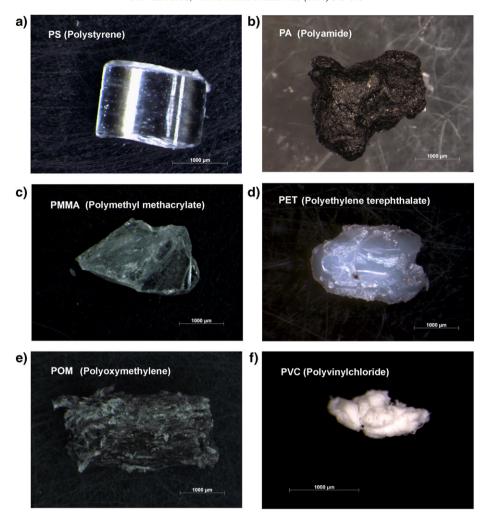| Polymer	Computer/Type	Density [kg m^{-3}]	Number	Size range [mm]	Sphericity	Flatness	Shape
PS	BASF 143 E, extruded and cutted	1050	60	1.6–1.8	0.48 (0.41–0.70)	1.34 (1.18–1.59)	Cylindrical
PA	BASF PA6 EXA® Mid	1140	90	1.3–0.36	0.52 (0.14–0.98)	1.25 (1.01–1.85)	Nodular
PMMA	PLEXIGLAS® 7 N Degussa	1190	134	0.5–2.3	0.60 (0.18–0.99)	1.41 (1.00–2.56)	Angular
PET	Bühler bottle grade recycled PET	1390	147	0.4–2.6	0.40 (0.12–0.96)	1.84 (1.02–4.78)	Angular
POM	DuPont Derlin® 100	1420	127	0.3–2.3	0.23 (0.03–0.86)	2.30 (1.05–5.29)	Angular
PVC	WestChemie Rigid-PVC Type 4122	1560	149	0.5–2.5	0.36 (0.08–0.83)	2.22 (1.10–6.14)	Nodular
ABS	Dow Chemical, Magnum 3404	1050					Nodular
HDPE	CS Plastik GmbH, Germany, pellets	955					Thin flakes
PET fibre	Trevira GmbH, Germany, yarn 110f96	1350					Elongate

Fig. 1. Images taken with stereo microscope showing exemplarily the polymer particles which were used in the sinking experiment: a) polystyrene (PS), b) polyamide (PA), c) polymethyl methacrylate (PMMA), d) polyethylene terephtalate (PET), e) polyoxymethylene (POM), f) polyvinylchloride (PVC).

V_s) which were calculated using the formula of Dietrich (1982):

$$theor. V_s = \left(\frac{\rho_s - \rho_f}{\rho_f} g v \omega_* \right)^{\frac{1}{3}} \qquad (3)$$

with ρ_s = particle density, ρ_f = fluid density, g = gravity of earth, v = kinematic viscosity, and ω_* = dimensionless sinking velocity. The values for fluid density and kinematic viscosity were taken from Feistel (2003) and Matthäus (1972), respectively. For a more detailed description of the calculation steps the authors refer to Dietrich (1982). It may be more common to use Stokes' law for the calculation of theoretical settling velocities of a perfect sphere in a fluid with laminar flow (e.g. Jähmlich et al., 2002; Ploug et al., 2008; Glockzin et al., 2014). However, Stokes' formula is assuming a very low Reynolds number which accounts for very small particles and thus, overestimates the sinking velocity of low-density spheres with diameters of >200 μm. That means for a sphere with a diameter of 1 mm a 10-fold overestimation (Gregory, 2006).

As the density of the 2 mm spheres differ slightly from the density of the spheres with size 0.5 mm the results have been adjusted to density 1050 kg m^{-3} by multiplying them with a correction factor. With this correction the measurements of the certified spheres fit very well the theoretical values as shown in Fig. 2 and more detailed in Table 2. Temperature was slightly varying during the experiments (av. temperature: 19.9 °C ± 1.2 °C), however no clear temperature depended behaviour

was recognized in the data as temperature induced variations are smaller than the variations occurring during measurements at similar temperature (Fig. 3).
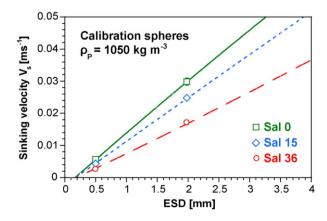

Fig. 2. Measured sinking velocities of certified calibration spheres with a diameter of 0.5 and 2 mm at salinity 0 (green square), 15 (blue diamond), and 36 (red circle) fitting the curves displaying calculated theoretical sinking velocities at salinity 0 (green solid line), 15 (blue short dashed line), and 36 (red long dashed line).

Table 2

Measured sinking velocities of certified calibration spheres (mean ± standard deviation, in brackets: n = number of measurements) with diameters 0.5 and 2.0 mm in comparison to theoretical values calculated after Dietrich (1982) at varying salinity (0, 15, and 36). Values marked with an asterisk are corrected by a factor as the density of the 2 mm spheres (1055 kg cm^{-3}) differ slightly from the density of the 0.5 mm spheres (1050 kg cm^{-3}). The water temperature is quoted as mean ± standard deviation.

Sphere ø [mm]	Salinity	Theor. $V_s \times 10^{-3}$ [ms^{-1}]	Measured $V_s \times 10^{-3}$ [ms^{-1}]	T [°C]
0.5	0	4.9	5.6 ± 0.5 (n = 37)	19.3 ± 1.3
	15	3.9	4.4 ± 0.3 (n = 43)	19.8 ± 1.3
	36	2.4	2.6 ± 0.3 (n = 41)	20.0 ± 1.1
2	0	30	30* ± 1.1 (n = 33)	19.7 ± 1.2
	15	25	25* ± 0.6 (n = 42)	20.6 ± 0.7
	36	17	17* ± 0.7 (n = 29)	20.5 ± 0.8

2.2. Aging experiments

2.2.1. Exposure to UV irradiation

To investigate the impact of UV irradiation, high-density polyethylene (HDPE), polystyrene (PS), acrylonitrile butadiene styrene (ABS), polyoxymethylene (POM), and PET fibres were exposed to the light of a metal vapour lamp (Lucky Reptile Bright Sun UV Desert) with UV fraction. The lamp was positioned 30 cm above the sample to enable an irradiation of UVA 17 Wm^{-2} and UVB 1 Wm^{-2} which approximates solar irradiance in late spring in middle Europe (e.g. Berlin in May 1990, UVA 17 Wm^{-2}, UVB 0.6 Wm^{-2}, Solar radiation data, SoDa Database) without exceeding a temperature of 30 °C. To study the effect of seawater in combination with UV exposure a further set of particles and fibres were stored in glass vials filled with artificial seawater (Sal 34, fill height 4 cm). Control samples with and without artificial seawater were kept in the dark. The particles and fibres surfaces were than investigated by SEM analysis (MERLIN VP compact, Carl Zeiss, Germany). Results presented here, are observations made after 40 days and a half year of 12 h daily UV exposure.

2.2.2. Mechanical stress

To simulate the effect of mechanical stress on microplastics in the surf zone polymer particles (HDPE, ABS, POM, and PET fibres) were filled into 250 mL glass bottles together with a mix of 200 g dwt. natural beach sand (natural organic matter has been removed before with 10% H_2O_2 at 50 °C) and Atlantic seawater (Sal 36). The bottles were fixed horizontally onto a laboratory orbital shaker (KS 501 digital, IKA-Werke GmbH & Co. KG, Germany) at 150 r min^{-1}. After 27 and 165 days, respectively, the particles and fibres were analysed by stereo microscope and SEM.

3. Results and discussion

3.1. Sinking velocities of different polymer particles as function of salinity, particle size, density and shape

Results of the sinking experiments with six different polymer types distinctly show the relevance of particle size, density and shape as well as salinity of the ambient fluid for the sinking velocity (Fig. 4). The particles ESD used in the experiment ranged between 0.3 and 3.6 mm and the sinking rates were between 6 and 91 × 10^{-3} ms^{-1}. PA exhibited the largest particles between 1.3 to 3.6 mm. The PS particles were quite equal ranging between 1.6 and 1.8 mm while the size ranges of PMMA, PET, POM, and PVC were 0.5–2.3 mm, 0.4–2.6 mm, 0.3–2.3 mm, and 0.5–2.5 mm, respectively. Similar size of microplastics debris (mean size 4.7 mm) was found at Califor-nian beaches (Ballent et al., 2013). Other publications (McDermid and McMullen, 2004; Browne et al., 2010) reported a major abundance of stranded microplastics with sizes <2.8 mm along the Pacific Ocean coasts. Smallest particles used in this study were 0.3 mm. Certainly, smaller fraction <0.3 mm is likely to be found and surely is of similar importance as it is small enough to be ingested by marine micro- and macroorganisms (e.g. Cole et al., 2011; Browne et al., 2008). The experimental investigation of this fraction is subject of a publication currently being in preparation as these microscopic particles demand other methods of investigation.

Because of the wider range of particle sizes the increase of settling velocities with particle size was clearly detectable. In the case of PS the particles showed no size dependent change due to their uniformity (mean ESD 1.7 mm, Fig. 4a). However, they elucidated very well the decrease of sinking velocity with increasing salinity (fluid density) having mean sinking rates of 17, 13, and 8 × 10^{-3} ms^{-1} at salinity 0, 15, and 36, respectively (Fig. 4a). In the cases of PA, PMMA, PET, POM and PVC (Fig. 4b–f) changing fluid density seemed to have just low impact on the sinking velocities due to distinctly higher particle densities compared to PS. Theoretical curves actually showed a decrease of salinity dependence with increasing particle density and mean values of the sinking velocities for Sal 0 to 36 were close to each other not showing such clear distinction as PS in Fig. 4a. In natural marine waters the density of seawater typically increases with depth. For example, in the stratified central Baltic Sea the upper surface layer has a salinity of about 6–8 while the salinity of the deep water layer is about 10–14 (Lass and Matthäus, 2008). Therefore, the particles should slow down with increasing depths possibly remaining floating when reaching a depth in which the water density is similar to the particle density (Wang et al., 2016). For larger particles with high densities (POM, PET, and PVC) as used in the experiments such salinity differences seem to be of no importance as they did not show significant slowing down with higher salinity (Fig. 4).
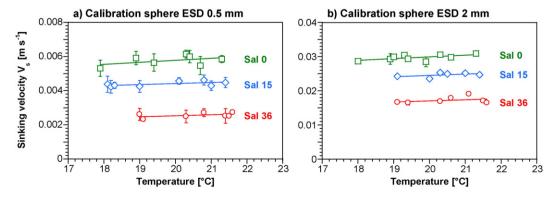

Fig. 3. Sinking velocities of certified calibration spheres with a diameter of a) 0.5 mm and b) 2 mm at salinity 0 (green squares), 15 (blue diamonds), and 36 (red circles) as a function of water temperature. The graph shows that temperature-dependent changes are smaller than the measuring variations at the same temperature as indicated by error bars.
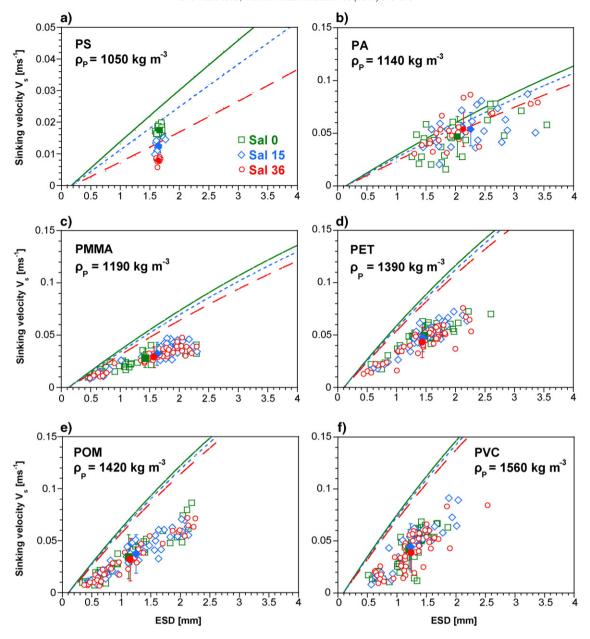
Fig. 4. Sinking velocities of a) PS, b) PA, c) PMMA, d) PET, e) POM, and f) PVC particles at salinity 0 (green squares), 15 (blue diamonds), and 36 (red circles). The particles vary in size as indicated by the equivalent spherical diameter (ESD) and in its density expressed as ρ_P. Theoretical sinking velocities calculated after Dietrich (1982) are displayed as green solid line for salinity 0, blue short dashed line for salinity 15, and red long dashed line for salinity 36.

A further influencing factor is the temperature. The experiments described here were conducted under approximately stable temperatures (19.9 °C ± 1.2 °C) but in temperate coastal waters like the Baltic Sea surface temperature can vary annually by around 15–16 °C (Matthäus, 1977). When assuming constant salinity the water density will increase with declining temperature generally reducing the sinking velocity of marine particles. That means a seasonal variation of microplastics sinking velocities being distinctly slower in the surface water during winter and also varying sinking velocities with depth due to temperature stratification of the water column. This is especially pronounced during the summer months due to for instance 10 °C higher temperatures in the surface water layer compared to the deep water in the central Baltic Sea (water depth approx. 250 m). In winter, conditions can change fundamentally with slightly lower water temperatures in the surface than in the deep water layer (Lass and Matthäus, 2008).

Surprisingly, the polymer particles did not show a clear distinction due to their particle density as it may be expected. Here, PA with the second lowest density of 1140 kg m^{-3} showed a higher mean sinking rate (50 × 10^{-3} ms^{-1}) than PVC (42 × 10^{-3} ms^{-1}) which had the highest particle density (1560 kg m^{-3}) of the polymers used in the experiment. This is not explained by a larger ESD of PA (mean ESD 2.1 mm) compared to PVC (mean ESD 1.2 mm) as PVC particles with that size should still be faster than those large PA particles only due to their density. The decisive factor here is the particle shape strongly affecting the sinking velocity of the particles. The particles shapes are described by the sphericity and flatness index (Table 1). A spheri-city index of 0 indicates non-sphericity, perfect spheres have an index of 1. Equant particles have a flatness index of 1 and the index becomes larger the flatter the particle is. The particles used in the experiments were far away from a perfectly spherical shape with moderate to low sphericity

indices (mean sphericity 0.23–0.60, Table 1) and being cylindrical (PS), nodular (PA, PVC), angular (PMMA, PET, and POM). The mean flatness indices ranged between 1.25 and 2.30 (Table 1). Therefore, the measured sinking rates (Fig. 4a, c–f) were usually markedly lower than the calculated theoretical rates based on perfectly rounded spheres (indicated by the lines in Fig. 4). The ratio between mean theoretical value and mean measured value revealed that the theoretical values for PS, PMMA, PET, POM, and PVC were around 2-fold higher than the measured rates (PS 1.75; PMMA 1.7, PET 1.8, POM 2.1, and PVC 2.1). However, smaller particles <1 mm approximated the theoretical curve while with growing particle size deviation from theoretical values was increasing as illustrated especially in Fig. 4c–e. This could be explained by a stronger drag force affecting larger particles and thus slowing them down. As shown by Komar and Reimers (1978) deviation from sphericity has a smaller effect on the sinking velocity of small particles but with increasing particles sizes the difference from the curve for perfect spheres is growing. The PA particles were closest to the theoretical values differing on average by a factor of 1.1 from the theoretical values. An explanation is the nodular, relatively rounded shape (Fig. 4b) resulting in a higher sphericity index (mean value 0.52) and concomitant low flatness index (mean value 1.25) compared to the other polymer types. Although, being quite rounded, PA showed a high variability in the sinking velocity which might be explained by slight changes of the particles density during the comminution process. In comparison, the higher flatness of PMMA particles (mean value 1.41) reduced the sinking velocities to values below PA despite their higher density (PA = 1140 kg m^{-3}, PMMA = 1190 kg m^{-3}). The low sphericity and relatively high flatness of PET (sphericity/flatness 0.40/1.84), POM (0.23/2.30), and PVC (0.36/2.22) leads to markedly slower sinking rates compared to the theoretical values. Deviation from a perfectly spherical shape causes a larger surface area inducing greater pressure and friction drag. When the particle is additionally flattened as especially in the cases of PET, POM, and PVC flow separation is induced which results in a higher drag coefficient and thus, reduction of the sinking velocity (Dietrich, 1982). Furthermore, irregularity of the shape may lead to instability in the particle motion affecting rotating, oscillating or tumbling of the particle which decreases the sinking velocity markedly (Dietrich, 1982). Thus, an oscillating motion could be observed during the settling of the cylindrical PS particles as has been described by Marchildon et al. (1964). The oblate POM particles showed a more chaotic settling motion often drifting into one direction as found by Field et al. (1997).

Information about the sinking behaviour of microplastics shall subsequently be implemented into model simulations estimating the residence time of the particles in the water column, their distribution and retention in the Baltic Sea. However, the findings in this section are only valid for new, non-aged particles which are recently released into the aquatic environment. When remaining there for a longer time, the particles undergo aging processes induced by different environmental factors which are discussed in the following section.

3.2. Environmental factors influencing the sinking behaviour of microplastics

Sinking experiments presented here were conducted with new non-aged microplastics. However, alteration of microplastics by weathering (UV radiation, biofouling, mechanical abrasion and shredding) has an impact on the physical properties (Morét-Ferguson et al., 2010) and thus, may also influence the sinking behaviour of the particles.

Therefore, plastic particles were exposed to mechanical and UV stress to study their modification. Mechanical abrasion may lead to shredding of particles into smaller pieces (Barnes et al., 2009). The experiments, however, revealed that the polymer particles are quite resistant and flexile against mechanical stress. After approximately one month of treatment just a rounding of particles was observed. This may lead on the one hand to a loss of mass and thus, a reduction of the particle density but on the other hand also to an enhancement of sinking velocity due to a higher degree of roundness (Powers, 1953). Furthermore, the attachment or incorporation of foreign particles as for instance clay minerals or quartz grains was observed (Fig. 5) which likewise may distinctly increase the sinking velocity of a particle.

Photodegradation and/or biological degradation may lead to a loss in weight and thus, decrease of the sinking velocity of particles. Laboratory experiments with UV radiation showed the so called yellowing of the ABS and PS particles (Fig. 6) being already visible after one month of UV treatment. Photodegradation is assumed to be caused by photo-Fries rearrangement which occurs at lower wavelengths (<290 mm) and generating yellow reaction products. At higher wavelength (330 mm) photooxidation is counteracting this process leading to bleaching of degraded compounds (Humphrey et al., 1973; Andrady et al., 1991). ABS and PS particles which were protected by a 4 cm water column of artificial seawater showed less discoloration but differences to completely exposed particles were just faintly visible. According to Andrady (2011) seawater decelerates photodegradation of floating plastic debris by about a factor of 10 compared to stranded plastics due to lower temperatures and oxygen concentration. The experiments presented here, however, showed that the yellowing process seems not to be influenced considerably by the artificial seawater. This may be due to relatively high temperatures of 30 °C which promote the photodegradation (Andrady, 2011). Furthermore, the vials used in the experiments were open to ambient air enabling the introduction of oxygen.

After a half year of irradiation the polymer particles did not exhibit visible structural changes at the surfaces. Exceptions were the PET fibres which showed the development of small pits with the first already occurring after one month of UV exposure (Fig. 6). Such structures have also been observed on plastic debris found at beaches of Hawaii (Corcoran et al., 2009; Cooper and Corcoran, 2010). Not clarified is the participation of microorganisms which are often found in or near such pits (Zettler et al., 2013; Reisser et al., 2014). As non-sterile artificial seawater was used in the experiments the existence of bacteria cannot be ruled out.

All in all, the qualitative investigation of UV treated and mechanically stressed polymer particles showed more or less visible structural changes (Figs. 5–7). Further investigation is needed examining the sinking rates of UV degraded and mechanically strained polymer particles to prove if differences to new, untreated particles are detectable.

On the other hand, development of biofilms on microplastics may alter the sinking behaviour considerably. Cózar et al. (2014) assumed that biofouling enhances microplastics densities to such an extent that particles with densities lower than the density of seawater (e.g. PE or PP) can reach densities which match or exceed seawater densities leading to slow sinking of the particles. This is in accordance to findings by Morét-Ferguson et al. (2010) who sampled polypropylene (PP) and polyethylene (PE) with distinctly increased particle densities in seawater of the western North Atlantic probably due to biofouling. Lobelle and Cunliffe (2011) additionally assumed that due to the development of biofilms the plastic particles may become less hydrophobic which facilitates their sinking. This may also explain the occurrence of PE and PP particles, which usually are just floating at the sea surface, in marine sediments as described e.g. by Vianello et al. (2013) and Dekiff et al. (2014). Furthermore, incorporation into organic aggregates may allow microscopic small plastic particles which do not sink due to their low density to reach the surface sediment (van Cauwenberghe et al., 2013). Long et al. (2015) detected the incorporation of 2 μm polystyrene spheres (density 1050 kg m^{-3}) in diatom aggregates using two different species and observing an increase or decrease of aggregate density with resulting acceleration or slowdown of the aggregates' sinking. Consequently, very small microplastics with particle densities close to seawater density may be able to sink down the water column probably slowing the aggregates down. In contrary, particles with distinctly
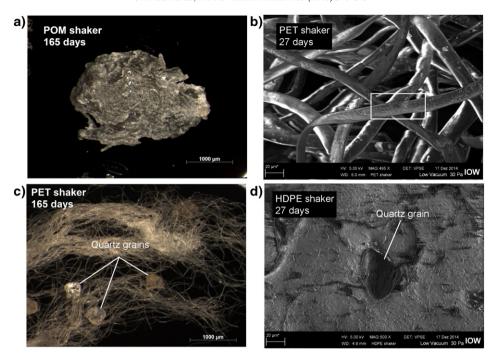
Fig. 5. Visible effects of mechanical stress on microplastic particles during the simulation of turbulent sand and seawater movement in the surf zone, a) stereo microscope image of a rounded POM particle after 165 days of treatment, b) SEM image of PET fibres showing surface abrasion after 27 days, c) stereo microscope image of PET fibres with incorporated quartz grains (after 165 days), and d) SEM image of the surface of a HDPE particle with attached quartz grain. SEM images were taken by R. Bahlo (IOW).

higher densities may enhance the aggregates density and thus their sinking velocity.

A further effective transport medium for microplastics may be faecal pellets. Cole et al. (2013, 2016) demonstrated that integration into co-pepod faecal pellets supports the vertical transfer of low-density microplastics. They furthermore showed that incorporated polystyrene spheres (size 7 and 21 μm) are able to alter the density and stability of the faecal pellets and slow down their sinking velocities.

3.3. Importance of microplastics for the marine matter flux

As shown in Table 3 the sinking velocities of microplastics presented in this study fit well to sinking velocities of beach debris HD pellets which were published by Ballent et al. (2013). Comparison to natural in-organic and organic marine particles indicates that microplastics with sizes >0.5 mm and densities which exceed the seawater density have
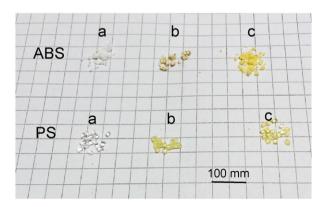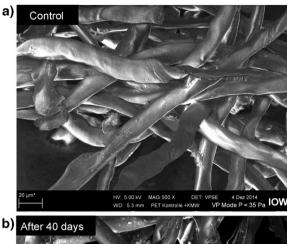

Fig. 6. UV experiment: Photographs of ABS (acrylonitrile butadiene styrene) particles and PS (polystyrene) particles which were a) stored in the dark, b) stored in artificial seawater (Sal 34, fill height 4 cm) and exposed 12 h daily to UV radiation, c) stored dry and treated 12 h daily with UV. The images were taken one year after start of the experiment showing significant yellowing of the particles b) and c) due to UV degradation.

distinctly higher sinking velocities than for instance clay or other mineral particles and aggregates. Exceptions are faecal pellets and quartz grains with high densities and ideal shapes leading to considerably faster sinking of those particles. Thus, the sinking velocities of the particles range between the values of faecal pellets reported by Yoon et al. (2001) and Cole et al. (2016) and quartz grains measured by Baba and Komar (1981).

Aggregates and faecal pellets fuel the biological carbon pump by transferring organic matter from the surface to the deep ocean (e.g. Turner, 2002). Organic-rich aggregates reveal high remineralisation rates with a carbon turnover rate of 8–9 days, already degrading during the transport into the deep ocean. Thus, about 80% of the carbon in small, slowly sinking aggregates is already decomposed during its way through a 200 m water column (Ploug et al., 1999). Faecal pellets may sink faster than aggregates but are assumed to degrade rapidly (e.g. Kiørboe, 2003; Ploug et al., 2008). Consequently, only a little percentage of net primary production reaches the deep sea and sea floor (e.g. Martin et al., 1987). As reported by e.g. Lobelle and Cunliffe (2011) and Zettler et al. (2013) plastic particles are quickly colonised by micro-organisms and act in that way as a further transport medium for organic carbon. It has been mentioned in the previous section that such biofilms are able to enhance the sinking velocities of microplastics markedly, thus, leading to the sinking of floating particles and transfer of the biofilm carbon to deeper water layers or the sediment.

The plastic particles investigated in this study may sink faster than a significant biofilm can develop on their surfaces. However, when considering those particles being deposited in coastal sediments, they underlie biofouling which is as effective as in the water column (Harrison et al., 2014). When now mobilised for instance during a storm event and spread from the coastal area into the open ocean (Ballent et al., 2013) they may sink quickly transporting the biofilm carbon to the sea floor where they are rapidly colonised by sediment bacteria (Harrison et al., 2014) which utilise the associated organic compounds. Thus, colonised sinking microplastics can influence the carbon pump especially in areas with high microplastics abundance as for instance in the subtropical gyres (Eriksen et al., 2014) contributing together with organic-rich aggregates and faecal pellets to the carbon
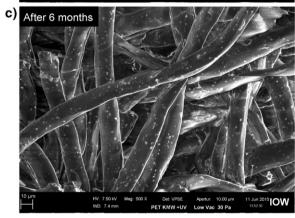
Fig. 7. UV experiment: SEM images of PET fibres a) without treatment (control), b) stored in artificial seawater (Sal 34, fill height 4 cm) after 40 days exposed to UV radiation. Small damages in the form of pits are visible. c) After 6 months of UV exposure the pits increased in size and quantity. SEM images were provided by R. Bahlo (IOW).

flux to the deep ocean and sediments. Further studies about degradation time of carbon on polymer particles are demanded to quantify the contribution of sinking fouled microplastics to the marine carbon flux.

4. Conclusions and outlook

The study presented here showed that not only the particle density but also especially the shape of the particles has a high influence on the sinking behaviour. Therefore, estimation of sinking velocities which are based on theoretical calculations assuming sinking of perfect spheres are inadequate and lead to strong deviation from the true sinking behaviour. Thus, the experimental studies of sinking behaviour are indispensable to provide appropriate data for model approaches simulating the distribution of microplastics in an aquatic system and

Table 3
Sinking velocities of polymer particles measured in this study (indicated by bold numbers) compared to published values of diverse marine particles varying in size and at different salinity.

Particles	Size [mm]	Salinity	$V_s \times 10^{-3}$ [m s^{-1}]	Reference
Clay minerals	<0.002	32.5	0.013–0.11	Whitehouse et al. (1958)
MnO$_x$ particles	0.016–0.02	~11	0.02–0.11	Glockzin et al. (2014)
Organic-rich aggregates	>0.05	av. 17	0.6–3	Jähmlich et al. (2002)
	1–3.2	32	1.1–5.8	Ploug et al. (2010)
	2.4–75	33	0.86 ± 0.45	Alldredge & Gottschalk (1988)
HD pellets	4.7 ± 0.3	36	28.2 ± 3.2	Ballent et al. (2013)
Polymer particles	**0.3–3.6**	**0, 15, 36**	**6–91**	**This study**
Faecal pallets	0.04–1.0	~35	0.3–14	Yoon et al. (2001)
Quartz grains	0.5–2.0	0	60–200	Baba & Komar (1981)

considering the physical properties of the water body (salinity and temperature) and hydrodynamic conditions (currents, tides, and waves).

In this study, new non-aged microplastics were observed to receive a basic understanding of the sinking behaviour of microplastics. However, previous publications and our observations showed that the particle density of microplastics are likely to be altered when exposed to weathering processes and biofouling which may lead to changes in the sinking velocities. Therefore, future work should consider using aged and fouled polymer particles to provide a more complete, close-to-nature documentation of the microplastics sinking behaviour.

Another point is the influence of microplastics on the marine carbon flux. Covered with a significant biofilm microplastics may be able to impact the transport of organic carbon to the deep sea or sediments. Further studies including budget calculations which estimate the transfer of organic carbon to deeper water layers and the sea floor via sinking microplastics may give some indication about the importance of microplastics for the marine carbon flux.

References

Alldredge, A.L., Gottschalk, C.C., 1988. Direct observations of the mass flocculation of diatom blooms: characteristics, settling velocities and formation of diatom aggregates. Deep Sea Res. Part A 36, 159–171.
Andrady, A.L., 2011. Microplastics in the marine environment. Mar. Pollut. Bull. 62, 1596–1605.
Andrady, A., Fueki, K., Torikai, A., 1991. Spectral sensitivity of polycarbonate to light-induced yellowing. J. Appl. Polym. Sci. 42, 2105–2107.
Baba, J., Komar, P.D., 1981. Measurements and analysis of settling velocities of natural quartz sand grains. J. Sediment. Petrol. 51, 631–640.
Bakir, A., Rowland, S.J., Thompson, R.C., 2014. Transport of persistent organic pollutants by microplastics in estuarine conditions. Estuar. Coast. Shelf Sci. 140, 14–21.
Bakir, A., Rowland, S.J., Thompson, R.C., 2012. Competitive sorption of persistent organic pollutants onto microplastics in the marine environment. Mar. Pollut. Bull. 64, 2782–2789.

Ballent, A., Pando, S., Purser, A., Juliano, M.F., Thomsen, L., 2013. Modelled transport of benthic marine microplastic pollution in the Nazaré Canyon. Biogeosciences 10, 7957–7970.

Barnes, D.K.A., Milner, P., 2005. Drifting plastic and its consequences for sessile organism dispersal in the Atlantic Ocean. Mar. Biol. 146, 815–825.

Barnes, D.K.A., Galgani, F., Thompson, R.C., Barlaz, M., 2009. Accumulation and fragmentation of plastic debris in global environments. Philos. Trans. R. Soc. B 364, 1985–1998.

Boerger, C.M., Lattin, G.L., Moore, S.L., Moore, C.J., 2010. Plastic ingestion by planktivorous fishes in the North Pacific Central Gyre. Mar. Pollut. Bull. 60, 2275–2278.

Browne, M.A., Crump, P., Niven, S.J., Teuten, E.L., Tonkin, A., Galloway, T., Thompson, R.C., 2011. Accumulations of microplastic on shorelines worldwide: sources and sinks. Environ. Sci. Technol. 45, 9175–9179.

Browne, M.A., Galloway, T., Thompson, R.C., 2010. Spatial patterns of plastic debris along estuarine shorelines. Environ. Sci. Technol. 44, 3404–3409.

Browne, M.A., Dissanayake, A., Galloway, T., Lowe, D.M., Thompson, R.C., 2008. Ingested microscopic plastic translocates to the circulatory system of the mussel, Mytilus edulis (L.). Environ. Sci. Technol. 42, 5026–5031.

Cailleux, A., 1945. Distinction des galets marins et fluviatiles. Bull. Soc. Geol. Fr. 15, 375–404.

Claessens, M., de Meester, S.D., van Landuyt, L., de Clerck, K., Janssen, C.R., 2011. Occurrence and distribution of microplastics in marine sediments along the Belgian coast. Mar. Pollut. Bull. 62, 2199–2204.

Cole, M., Lindeque, P., Fileman, E., Clark, J., Lewis, C., Halsband, C., Galloway, T.S., 2016. Microplastics alter the properties and sinking rates of zooplankton faecal pellets. Environ. Sci. Technol. 50, 3239–3246.

Cole, M., Lindeque, P., Fileman, E., Halsband, C., Goodhead, R., Moger, J., Galloway, T.S., 2013. Microplastic ingestion by zooplankton. Environ. Sci. Technol. 47, 6646–6655.

Cole, M., Lindeque, P., Halsband, C., Galloway, T.S., 2011. Microplastics as contaminants in the marine environment: a review. Mar. Pollut. Bull. 62, 2588–2597.

Collignon, A., Hecq, J.-H., Glagani, F., Voisin, P., Collard, F., Goffart, A., 2012. Neustonic microplastic and zooplankton in the north western Mediterranian Sea. Mar. Pollut. Bull. 64, 861–864.

Cooper, D.A., Corcoran, P.L., 2010. Effects of mechanical and chemical processes on the degradation of plastic beach debris on the island of Kauai, Hawaii. Mar. Pollut. Bull. 60, 650–654.

Corcoran, P.L., Biesinger, M.C., Grifi, M., 2009. Plastics and beaches: a degrading relationship. Mar. Pollut. Bull. 58, 80–84.

Cózar, A., Echevarria, F., González-Gordillo, I.J., Irigoien, X., Úbeda, B., Hernández-León, S., Palma, A.T., Navarro, S., García-de-Lomas, J., Ruiz, A., Fernández-de-Puelles, M.L., Duarte, C.M., 2014. Plastic debris in the open ocean. Proc. Natl. Acad. Sci. 111, 10239–10244.

Davison, P., Asch, R.G., 2011. Plastic ingestion by mesopelagic fishes in the North Pacific subtropical gyre. Mar. Ecol. Prog. Ser. 432, 173–180.

Dekiff, J.H., Remy, D., Klasmeier, J., Fries, E., 2014. Occurrence and spatial distribution of microplastics in sediments from Norderney. Environ. Pollut. 186, 248–256.

Derraik, J.G.B., 2002. The pollution of the marine environment by plastic debris: a review. Mar. Pollut. Bull. 44, 842–852.

Desforges, J.P., Galbraith, M., Ross, P.S., 2015. Ingestion of microplastics by zooplankton in the Northeast Pacific Ocean. Arch. Environ. Contam. Toxicol. 69, 320–330.

Dietrich, W.E., 1982. Settling velocity of natural particles. Water Resour. Res. 18 (6), 1615–1626.

Dimitrakakis, E., Janz, A., Bilitewski, B., Gidarakos, E., 2009. Determination of heavy metals and halogens in plastics from electric and electronic waste. Waste Manag. 29 (10), 2700–2706.

Endo, S., Takizawa, R., Okuda, K., Takada, H., Chiba, K., Kanehiro, H., Ogi, H., Yamashita, R., Date, T., 2005. Concentration of polychlorinated biphenyls (PCBs) in beached resin pellets: variability among individual particles and regional differences. Mar. Pollut. Bull. 50, 1103–1114.

Eriksen, M., Lebreton, L.C.M., Carson, H.S., Thiel, M., Moore, C.J., Borerro, J.C., Galgani, F., Ryan, P.G., Reisser, J., 2014. Plastic pollution in the world's oceans: more than 5 trillion plastic pieces weighing over 250,000 tons afloat at sea. PLoS One 9, 1–15.

Feistel, R., 2003. A new extended Gibbs thermodynamic potential of seawater. Prog. Oceanogr. 58 (1), 43–114.

Field, S.B., Klaus, M., Moore, M.G., Nori, F., 1997. Chaotic dynamics of falling disks. Nature 388, 252–254.

Galgani, F., Hanke, G., Werner, S., de Vrees, L., 2013. Marine litter within the European marine strategy framework directive. ICES J. Mar. Sci. 70 (6), 1055–1064.

GESAMP, 2015. Sources, Fate and Effects of Microplastics in the Marine Environment: A Global Assessment. In: Kershaw, P.J. (Ed.), IMO/FAO/UNESCO-IOC/UNIDO/WMO/IAEA/UN/UNEP/UNDP Joint Group of Experts on the Scientific Aspects of Marine Environmental Protection. Reports and Studies Series, GESAMP No. 90 (96 p.).

Glockzin, M., Pollehne, F., Dellwig, O., 2014. Stationary sinking velocity of authigenic manganese oxides at pelagic redoxclines. Mar. Chem. 160 (76-74).

Gregory, J., 2006. Particles in Water - Properties and Processes. Taylor & Francis Group, London, New York (173 p.).

Harrison, J.P., Schratzberger, M., Sapp, M., Osborn, A.M., 2014. Rapid bacterial colonization low-density polyethylene microplastics in coastal sediment microcosms. BMC Microbiol. 14, 232.

Holmes, L.A., Turner, A., Thompson, R.C., 2012. Adsorption of trace metals to plastic resin pellets in the marine environment. Environ. Pollut. 160, 42–48.

Humphrey, J.S., Shultz, A.R., Jacquiss, D.B.G., 1973. Flash photochemical studies of polycarbonate and related model compounds, photodegradation vs. photo-fries rearrangement. Macromolecules 6, 305–314.

Ivar do Sul, J.A., Costa, M.F., 2007. Marine debris review for Latin America and the wider Caribbean region: from the 1970s until now, and where do we go from here? Mar. Pollut. Bull. 54, 1087–1104.

Jähmlich, S., Lund-Hansen, L.C., Leipe, T., 2002. Enhanced settling velocities and vertical transport of particulate matter by aggregation in the benthic boundary layer. Dan. J. Geogr. 102, 37–49.

Kiørboe, T., 2003. High turnover rates of copepod fecal pellets due to Noctiluca scintillans grazing. Mar. Ecol. Prog. Ser. 258, 181–188.

Koelmans, A.A., Besseling, E., Foekema, E.M., 2014. Leaching of plastic additives to marine organisms. Environ. Pollut. 187, 49–54.

Komar, P.D., Reimers, C.E., 1978. Grain shape effects on settling rates. J. Geol. 86, 193–209.

Kukulka, T., Proskurowski, G., Morét-Ferguson, S., Meyer, D.W., Law, K.L., 2012. The effect of wind mixing on the vertical distribution of buoyant plastic debris. Geophys. Res. Lett. 39 (7), 1–6.

Krumbein, W.C., 1941. Measurement and geological significance of shape and roundness of sedimentary particles. J. Sediment. Petrol. 11, 64–72.

Kumar, R.G., Strom, K.B., Keyvani, A., 2010. Floc properties and settling velocity of San Jacinto estuary mud under variable shear and salinity conditions. Cont. Shelf Res. 30, 2067–2081.

Lass, H.-U., Matthäus, W., 2008. General Oceanography of the Baltic Sea. In: Feistel, R., Nausch, G., Wasmund, N. (Eds.), State and Evolution of the Baltic Sea, 1952–2005. John Wiley & Sons, Hoboken, New Jersey, p. 703.

Liebezeit, G., Dubaish, F., 2012. Microplastics in beaches of the east Frisian Islands Spiekeroog and Kachelotplate. Bull. Environ. Contam. Toxicol. 89, 213–217.

Lithner, D., Larsson, Å., Dave, G., 2011. Environmental and health hazard ranking and assessment of plastic polymers based on chemical composition. Sci. Total Environ. 409, 3309–3324.

Lobelle, D., Cunliffe, M., 2011. Early microbial biofilm formation on marine plastic debris. Mar. Pollut. Bull. 62 (1), 197–200.

Long, M., Moriceau, B., Gallinari, M., Lambert, C., Huvet, A., Raffray, J., Soudant, P., 2015. Interactions between microplastics and phytoplankton aggregates: impact on their respective fates. Mar. Chem. 175, 39–46.

Marchildon, E.K., Clamen, A., Gauvin, W.H., 1964. Drag and oscillatory motion of freely falling cylindrical particles. Can. J. Chem. Eng. 42, 178–182.

Martin, J.H., Knauer, G.A., Karl, D.M., Broenkow, W.W., 1987. VERTEX: carbon cycling in the Northeast Pacific. Deep-Sea Res. 34, 267–285.

Mato, Y., Isobe, T., Takada, H., Kanehiro, H., Ohtake, C., Kaminuma, T., 2000. Plastic resin pellets as a transport medium for toxic chemicals in the marine environment. Environ. Sci. Technol. 35 (2), 318–324.

Matthäus, W., 1977. Zur mittleren jahreszeitlichen Veränderlichkeit der Temperatur in der offenen Ostsee. Beitr. Meereskun. 40, 117–155.

Matthäus, W., 1972. Die Viskosität des Meerwassers. Beitr. Meereskun. 29, 48–66.

McCormick, A., Hoellein, T.J., Mason, S.A., Schluep, J., Kelly, J.J., 2014. Microplastic is an abundant and distinct microbial habitat in an urban river. Environ. Sci. Technol. 48, 11863–11871.

McDermid, K.J., McMullen, T.L., 2004. Quantitative analysis of small-plastic debris on beaches in the Hawaiian archipelago. Mar. Pollut. Bull. 48, 790–794.

Morét-Ferguson, S., Law, K.L., Proskurowski, G., Murphy, E.K., Peacock, E.E., Reddy, C.M., 2010. The size, mass, and composition of plastic debris in the western North Atlantic Ocean. Mar. Pollut. Bull. 60 (10), 1873–1878.

Oberbeckmann, S., Löder, M.G.J., Labrenz, M., 2015. Marine microplastic-associated biofilms – a review. Environ. Chem. 12, 551–562.

Pegram, J.E., Andrady, A.L., 1989. Outdoor weathering of selected polymeric materials under marine exposure conditions. Polym. Degrad. Stab. 26 (4), 333–345.

Ploug, H., Terbrüggen, A., Kaufmann, A., Wolf-Gladrow, D., Passow, U., 2010. A novel method to measure particle sinking velocity in vitro, and its comparison to three other in vitro methods. Limnol. Oceanogr. Methods 8, 386–393.

Ploug, H., Iversen, M.H., Koski, M., Buitenhuis, E.T., 2008. Production, oxygen respiration rates, and sinking velocity of copepod fecal pellets: direct measurements of ballasting by opal and calcite. Limnol. Oceanogr. 53 (2), 469–476.

Ploug, H., Grossart, H.-P., Azam, F., Jørgensen, B.B., 1999. Photosynthesis, respiration, and carbon turnover in sinking marine snow from surface waters of Southern California Bight: implications for the carbon cycle in the ocean. Mar. Ecol. Prog. Ser. 179, 1–11.

Powers, M.C., 1953. A new roundness scale for sedimentary particles. J. Sediment. Petrol. 23 (2), 117–119.

Reisser, J., Shaw, J., Hallegraeff, G., Proietti, M., Barnes, D.K.A., 2014. Millimeter-sized marine plastic: a new pelagic habitat for microorganisms and invertebrates. PLoS One 9 (6), e100289.

Sadri, S.S., Thompson, R.C., 2014. On the quantity and composition of floating plastic debris entering and leaving the Tamar Estuary, Southwest England. Mar. Pollut. Bull. 81, 55–60.

Shaw, D.G., Day, R.H., 1994. Colour- and form-dependent loss of plastic micro-debris from the North Pacific Ocean. Mar. Pollut. Bull. 28, 39–43.

Stolte, A., Forster, S., Gerdts, G., Schubert, H., 2015. Microplastic concentrations in beach sediments along the German Baltic coast. Mar. Pollut. Bull. 99, 216–229.

Teuten, E.L., Saquing, J.M., Knappe, D.R.U., Barlaz, M.A., Jonsson, S., Björn, A., Rowland, S.J., Thompson, R.C., Galloway, T.S., Yamashita, R., Ochi, D., Watanuki, Y., Moore, C., Viet, P.H., Tana, T.S., Prudente, M., Boonyatumanond, R., Zakaria, M.P., Akkhavong, K., Ogata, Y., Hirai, H., Iwasa, S., Mizukawa, K., Hagino, Y., Imamura, A., Saha, M., Takada, H., 2009. Transport and release of chemicals from plastics to the environment and to wildlife. Philos. Trans. R. Soc. B 364, 2027–2045.

Thiel, M., Hinojosa, I., Vásquez, N., Macaya, E., 2003. Floating marine debris in coastal waters of the SE-Pacific (Chile). Mar. Pollut. Bull. 46 (2), 224–231.

Thompson, R.C., Moore, C., Andrady, A., Gregory, M., Takada, H., Weisberg, S., 2005. New directions in plastic debris. Science 310, 1117.

Turner, A.T., Holmes, L.A., 2015. Adsorption of trace metals by microplastic pellets in fresh water. Environ. Chem. 12 (5), 600–610.

Turner, J.T., 2002. Zooplankton fecal pellets, marine snow and sinking phytoplankton blooms. Aquat. Microb. Ecol. 27, 57–102.

Van Cauwenberghe, L., Claessens, M., Vandegehuchte, M.B., Mees, J., Janssen, C.R., 2014. Assessment of marine debris on the Belgian continental shelf. Mar. Pollut. Bull. 73, 161–169.

Van Cauwenberghe, L., Vanreusel, A., Mees, J., Janssen, C.R., 2013. Microplastic pollution in deep-sea sediments. Environ. Pollut. 182, 495–499.

Vianello, A., Boldrin, A., Guerriero, P., Moschino, V., Rella, R., Sturaro, A., Da Ros, L., 2013. Microplastic particles in sediments of lagoon of Venice, Italy: first observations on occurrence, spatial patterns and identification. Estuar. Coast. Shelf Sci. 130, 54–61.

Wang, J., Tan, Z., Peng, J., Qiu, Q., Li, M., 2016. The behaviors of microplastics in the marine environment. Mar. Environ. Res. 113, 7–17.

Whitehouse, U.G., Jeffrey, L.M., Debbrecht, J.D., 1958. Differential Settling Tendencies of Clay Minerals in Saline Waters. Clays and Clay Minerals: Proceedings of the Seventh National Conference on Clays and Clay Minerals. Pergamon Press, pp. 1–79.

Yoon, W.D., Kim, S.K., Han, K.N., 2001. Morphology and sinking velocities of fecal pellets of copepod, molluscan, euhpausiid, and salp taxa in the northeastern tropical Atlantic. Mar. Biol. 139, 923–928.

Zettler, E.R., Mincer, T.J., Amaral-Zettler, L.A., 2013. Life in the "plastisphere": microbial communities on plastic marine debris. Environ. Sci. Technol. 47, 7137–7146.

Zhao, S., Zhu, L., Wang, T., Li, D., 2014. Suspended microplastics in the surface water of the Yangtze estuary system, China: first observations on occurrence, distribution. Mar. Pollut. Bull. 86, 562–568.